JOURNAL OF PHYSICAL ORGANIC CHEMISTRY
J. Phys. Org. Chem. 2005; **18:** 498–503
Published online 1 February 2005 in Wiley InterScience (www.interscience.wiley.com). DOI: 10.1002/poc.900

Multiple-substituent effects on the isomerization of unsymmetrical *cis*-1,3-diphenyltriazenes

Huaibin Zhang and Mónica Barra*

Department of Chemistry, University of Waterloo, Waterloo, Ontario, Canada N2L 2G1

Received 9 September 2004; revised 10 November 2004; accepted 22 November 2004

ABSTRACT: *Trans*-to-*cis* photoisomerization of unsymmetrical 4,4′-disubstituted *trans*-1,3-diphenyltriazenes renders a non-equilibrium mixture of two isomeric *cis* pairs which, as in the case of symmetrical 1,3-diphenyltriazenes, undergo thermal *cis*-to-*trans* isomerization by means of 1,3-prototropic rearrangements catalyzed by general acids and general bases. A quantitative analysis, by means of a multiple-substituent Hammett equation, of the rate constants for restricted rotation around the N-2—N-3 bond in *cis*-1,3-diphenyltriazenes renders ρ values of -1.93 ± 0.08 and 0.82 ± 0.08 for N-1 and N-3, respectively. Copyright © 2005 John Wiley & Sons, Ltd.
Supplementary electronic material for this paper is available in Wiley Interscience at http://www.interscience.wiley.com/jpages/0894-3230/suppmat/

KEYWORDS: triazenes; geometrical isomerism; restricted rotation; substituent effects; Hammett equation

INTRODUCTION

Unsaturated compounds able to undergo light-induced reversible changes in double-bond configuration are subjects of interest for potential applications, among others, in information storage systems and in (supra)molecular switching devices.[1,2] In contrast to the case of azo compounds, ones of the most thoroughly studied photochromic materials with nitrogen-containing π-systems[2] (the detailed literature on photoisomerization mechanistic studies of azo compounds is beyond the scope of this paper; only a few representative and recent articles are listed here[3]), very limited information is available regarding the geometrical isomerization mechanism for triazenes,[4–7] compounds characterized by having a diazoamino group (i.e.—$N^1=N^2—N^3<$) and of potential use as optical memory materials for photo-mode recording.[8] In an effort to provide a framework for the understanding of the factors that govern the geometrical isomerization of triazenes, and that ultimately determine the usefulness of these compounds as photochromic materials, recent investigations in our laboratory have focused on the *cis*-to-*trans* isomerization mechanism of symmetrical 4,4′-disubstituted 1,3-diphenyltriazenes (**DPT**).[6,7] It has been indicated that photoinduced *trans*-to-*cis* isomerization, via laser-flash excitation of *trans*-**DPT** in aqueous media, renders a non-equilibrium mixture of *s-cis* and *s-trans* conformers of the corresponding *cis*-**DPT**;[6,7] the *cis-s-trans* conformers subsequently revert to the thermodynamically more stable *trans* forms via an acid/base-catalyzed 1,3-prototropic rearrangement (Scheme 1).[6,7] Acid catalysis (attributed to rate-limiting proton transfer to N-1) becomes predominant as the electron-donating character of the aryl groups increases, whereas base catalysis (attributed to rate-limiting base promoted ionization of N-3) becomes dominant as the electron-withdrawing character of the aryl groups increases.[7] Interestingly, the process ascribed to *cis-s-cis* to *cis-s-trans* conversion (i.e. restricted rotation around the N-2—N-3 bond) becomes rate controlling when working in aqueous NaOH solutions.[6,7] Furthermore, the rate constants ascribed to restricted rotation have been shown to increase as the ability of the aryl groups to withdraw electrons also increases, which implies the intramolecular process to be more susceptible to the electronic character of the aryl group attached to N-1 than of that bonded to N-3.[7]

Evidently, an additional aspect arises when unsymmetrical disubstituted *trans*-1,3-diphenyltriazenes are considered, since in essence they exist as a pair of distinguishable tautomeric isomers [Eqn (1)].[9–11] Hence one would anticipate that *trans*-to-*cis* photoisomerization of unsymmetrical *trans*-**DPT** would render a non-equilibrium mixture of *two* pairs of *cis* isomers, i.e. one pair of *cis*-conformers per tautomeric *trans* form.

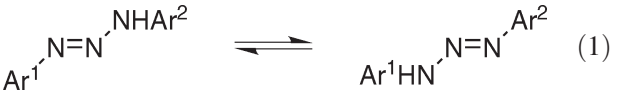

(1)

**Correspondence to:* M. Barra, Department of Chemistry, University of Waterloo, 200 University Avenue West, Waterloo, Ontario, Canada N2L 2G1.
E-mail: mbarra@sciborg.uwaterloo.ca
Contract/grant sponsor: Natural Sciences and Engineering Research Council (NSERC) of Canada.

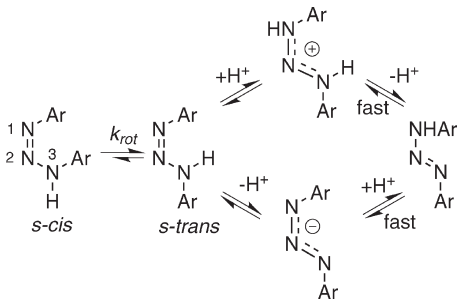

Scheme 1

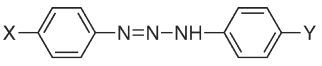

Triazene	X	Y
MHDPT	CH_3O	H
FHDPT	CF_3	H
MFDPT	CH_3O	CF3

Scheme 2

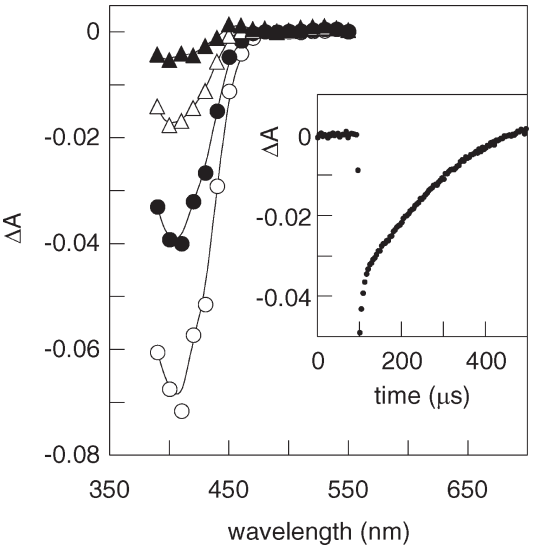

Figure 1. Transient absorption spectra for **FHDPT** (in NaOH solution) obtained 14 (○), 128 (●), 260 (△) and 372 μs (▲) after laser pulse at pH 13.53. Inset: kinetic trace recorded at 390 nm (pH 13.99)

In this paper, we report the results of a study on the thermal *cis*-to-*trans* isomerization of a set of unsymmetrical 4,4′-disubstituted-1,3-diphenyltriazenes (Scheme 2) (for convenience of notation, unsymmetrical 4,4′-disubstituted-1,3-diphenyltriazenes are referred by a single name, although, as shown in Eqn (1) and discussed later, these substances exist as a mixture of tautomeric isomers) to probe the implications of tautomeric isomerism on the geometrical isomerization mechanism illustrated in Scheme 1, and, in particular, to characterize further the influence of aryl substitution on the N-2—N-3 rotational barrier.

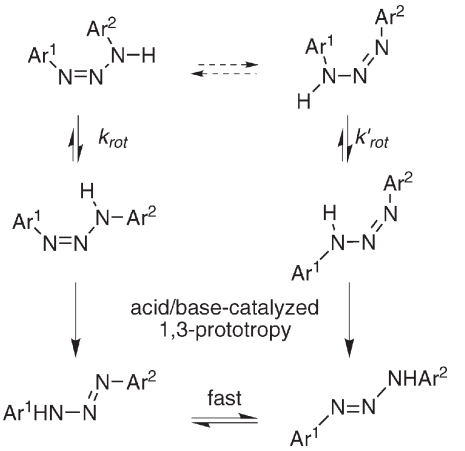

Scheme 3

RESULTS AND DISCUSSION

In agreement with previous studies on symmetrical 4,4′-disubstituted-1,3-diphenyltriazenes, laser excitation (at $\lambda = 355$ nm) of aqueous solutions of the *trans* forms of any of the compounds shown in Scheme 2 leads to an instantaneous decrease in the absorbance of the solution (bleaching), owing to photoinduced *trans*-to-*cis* isomerization (Fig. 1 is representative). In all cases, this instantaneous bleaching is followed by complete recovery of the initial absorbance of the solution, owing to thermal *cis*-to-*trans* isomerization (Fig. 1, inset). Recovery traces were collected for each of the compounds shown in Scheme 2 as a function of pH and buffer concentration. In most cases, recovery traces are very well reproduced by a biexponential function (Tables S1–S20, available as Supplementary Material at Wiley Interscience). The fact that two kinetic processes are being observed indicates the presence of (at least) two absorbing species of different reactivity. These two kinetic processes can be attributed to the presence of two pairs of *cis* isomers (i.e. one pair of *cis*-conformers per tautomeric *trans* form) that isomerize at different rates. This assumption requires the *cis-s-cis* isomers to be linked through a 'slow' tautomeric equilibrium (Scheme 3), i.e. the *cis-s-cis* interconversion step is assumed to act as an insulator between the two (rapid) *cis*-to-*trans* isomerization reactions, thereby making them independent of each other. This seems reasonable considering that, unlike tautomerization between *cis-s-cis* isomers, restricted rotation around the N-2—N-3 bond and 1,3-prototropy of *cis-s-trans* isomers significantly decrease the steric hindrance between phenyl rings.

Consistent with previous observations for symmetrical 1,3-diaryltriazenes, it is found that the observed rate constants determined in acetate, phosphate, carbonate and piperidine buffers vary with pH and buffer concentration (Tables S1–S3, S5–S13 and S15–S19, available as Supplementary Material at Wiley Interscience). The buffer dependence plots (Fig. 2 is representative) are fairly linear, hence data are interpreted in terms of

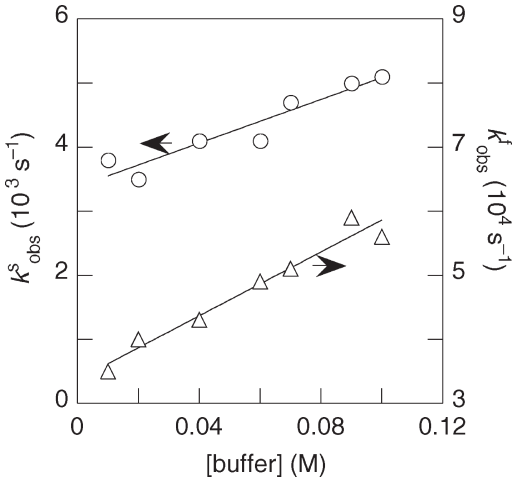

Figure 2. Buffer concentration dependence of the observed rate constants for **FHDPT** *cis*-to-*trans* isomerization in acetate buffer at pH = 4.96 (k^s and k^f refer to the rate constants for the slower and faster processes, respectively)

Eqn (2), where k_0 represents the rate constant for reaction through solvent-related species and k_B represents the buffer rate constant.

$$k_{obs} = k_0 + k_B[\text{buffer}] \quad (2)$$

The resulting k_0 values, together with the k_{obs} values obtained in NaOH solutions (Tables S4, S14 and S20, available as Supplementary Material at Wiley Interscience), are used to build the pH–rate profiles shown in Fig. 3. Based on the mechanism presented in Scheme 3, if the *cis-s-cis* interconversion step acts as an insulator between the two (rapid) *cis*-to-*trans* isomerization reactions, one would expect the pH–rate profile of each substrate to be characterized by two curves, each curve representing the isomerization of one of the two pairs of *cis*-conformers. According to Scheme 3, and the pH–rate profiles reported for symmetrical triazenes,[6,7] each of these curves should be characterized by a V-shaped profile (corresponding to rate-limiting acid/base-catalyzed 1,3-prototropy) that levels off at both high and low pHs as a result of a change in rate-controlling step (i.e. rate-limiting restricted rotation). The empirical rate law for the V-shaped profile is $k_0 = c_1[H^+] + c_2 + c_3[HO^-]$, where c_1, c_2 and c_3 represent the rate coefficients for 1,3-prototropy assisted by protons, water molecules and hydroxide anions, respectively. A theoretical fit of the data to this equation has not been done because in no case could the rates of *cis*-to-*trans* isomerization for the corresponding two pairs of *cis*-conformers be experimentally distinguished in the range $6 < pH < 10$. It should be pointed out that such a fitting has been reported for 1,3-diphenyltriazene, demonstrating that the resulting rate coefficients c_1 and c_3 are consistent with diffusion-controlled protonation rate constants.[6] Two V-shaped curves are clearly seen in the case of **FHDPT** [Fig. 3(B)]. [Triazenes are very sensitive to acids, decomposing in aqueous media to nitrogen, amines and alcohols. Among the three target

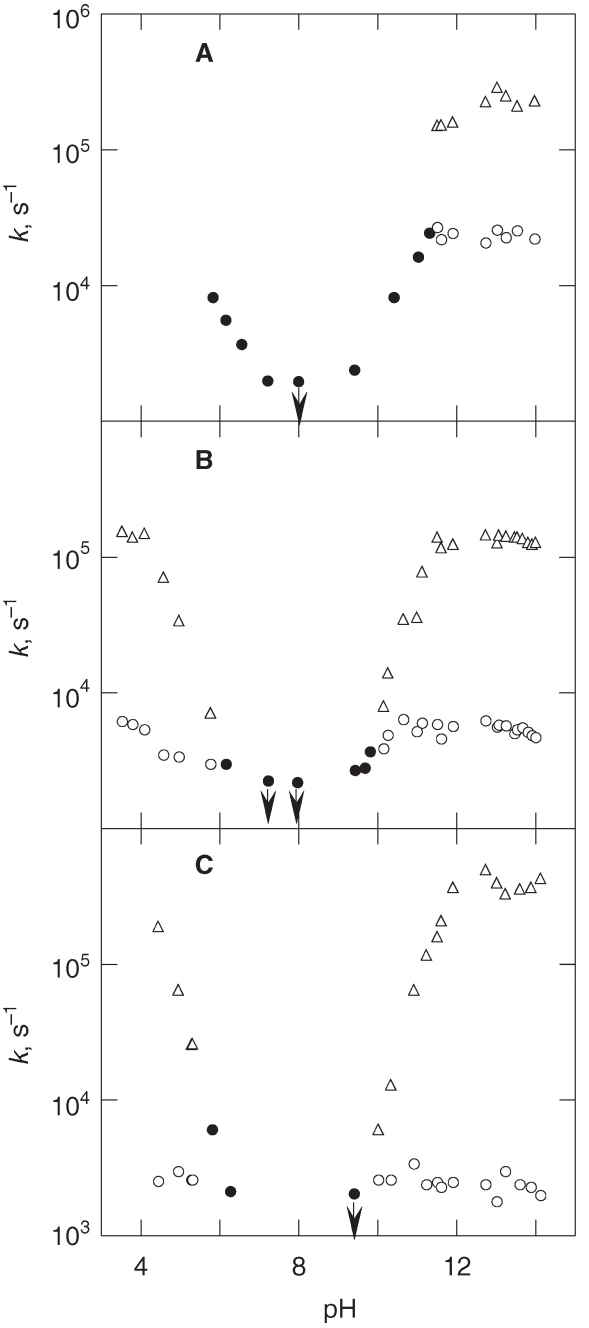

Figure 3. Plots of rate constants (extrapolated to zero buffer concentration) vs pH for *cis*-to-*trans* isomerization of **MHDPT** (A), **FHDPT** (B) and **MFDPT** (C), obtained from mono- (●) and biexponential (△, ○) kinetic traces. Arrows indicate direction of possible movement of points, which are maximum values (the slowest rate constant that can be determined with our laser-flash photolysis system is $\sim 2000\ s^{-1}$)

substrates, **FHDPT** is the most stable ($k_{decomposition} = 0.30 \pm 0.02$, 1.78 ± 0.05, and $131 \pm 2\ M^{-1}\ s^{-1}$ for **FHDPT**, **MFDPT** and **MHDPT**, respectively), which allows us to carry out experiments in a wider range of pH than in the case of the other two substrates.] For **MHDPT** [Fig. 3(A)], a single kinetic process is observed under the experimental conditions where the 1,3-prototropic rearrangements are

rate-controlling, in agreement with the expectation that the rates of *cis*-to-*trans* isomerization for the two isomeric *cis-s-trans* **MHDPT** forms are similar [as inferred from the rate constants previously obtained for 1,3-bis(4-methoxyphenyl)triazene and 1,3-diphenyltriazene],[7] and therefore too close to be distinguished kinetically. In the case of **MFDPT** [Fig. 3(C)], the resulting pH–rate profile clearly indicates that the rate of isomerization attributed to one of the *cis* pairs is pH independent, which would indicate that for this *cis* pair restricted rotation around the N-2—N-3 bond is the rate-limiting step under all the experimental conditions of this study. It should also be noted that these values are fairly close to the detection limit of our equipment (the slowest rate constant that can be determined with our laser-flash photolysis system is $\sim 2000\,s^{-1}$) and should therefore be used with caution.

The main question for all three pH–rate profiles is which *cis* pair corresponds to each curve. As shown in Fig. 3, two pH-independent processes are observed in NaOH solutions with all three substrates. These pH-independent processes are attributed to rate-limiting restricted rotation around the N-2—N-3 bond of *cis-s-cis* tautomers that clearly undergo rotation at different rates. Restricted rotation around the N-2—N-3 bond of triazenes can be explained in terms of a 1,3-dipolar resonance model, as shown in Eqn (3).

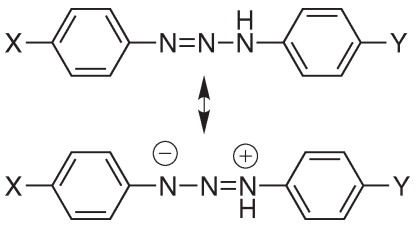

(3)

Table 1. Rate constants for restricted rotation

Triazene		X[a]	Y[a]	k_{rot} (s^{-1})
MHDPT	(a)	CH_3O	H	$(2.4 \pm 0.2) \times 10^5$
	(b)	H	CH_3O	$(2.33 \pm 0.08) \times 10^4$
FHDPT	(a)	H	CF_3	$(1.4 \pm 0.1) \times 10^5$
	(b)	CF_3	H	$(5.4 \pm 0.2) \times 10^3$
MFDPT	(a)	CH_3O	CF_3	$(4 \pm 3) \times 10^5$
	(b)	CF_3	CH_3O	$(2.6 \pm 0.3) \times 10^3$

[a] The positions of X and Y are given in Eqn (3).

Based on this model, the more stable the charges on the 1,3-dipolar resonance form are, the lower the corresponding rate constant for restricted rotation is. Hence the resulting rate constants values for restricted rotation for each substrate are assigned to the corresponding tautomeric forms as indicated in Table 1.

As mentioned earlier, the observed rate constants determined in acetate, phosphate and carbonate buffers (i.e. conditions under which the 1,3-prototropic rearrangement is rate controlling) vary with pH and buffer concentration. The k_B values obtained according to Eqn (2), if at all significant, are summarized in Table 2. Values for acetate and phosphate buffers are found to increase with decreasing pH (indicative of general acid catalysis), whereas those for carbonate buffer increase with increasing pH (indicative of general base catalysis). Based on the assignments given in Table 1, the k_B values listed for **FHDPT** and **MFDPT** in Table 2 would correspond to 1,3-prototropy of the *cis-s-trans* isomers of type (a) [i.e. $Y = CF_3$ in Eqn (3)]. Although the number of data points per class of buffer is limited for a quantitative analysis, it is interesting that the pH dependence of the k_B values obtained for acetate buffer indicates that the

Table 2. Buffer rate constants (k_B) for *cis*-to-*trans* isomerization of unsymmetrical 4,4′-disubstituted-1,3-diphenyltriazenes in buffered aqueous solution[a]

MHDPT[b]		**FHDPT**[c]		**MFDPT**[c]	
pH	k_B[d] ($10^4\,M^{-1}\,s^{-1}$)	pH	k_B[d] ($10^5\,M^{-1}\,s^{-1}$)	pH	k_B[d] ($10^5\,M^{-1}\,s^{-1}$)
5.82[e]	7.0 ± 0.8	4.08[f]	4 ± 2	4.44[f]	5.7 ± 0.7
6.14[e]	5.1 ± 0.8	4.57[f]	3.1 ± 0.9[g]	4.94[f]	3.8 ± 0.3
6.54[e]	3.3 ± 0.3	4.96[f]	2.5 ± 0.2[h]	5.28[f]	3.0 ± 0.1
7.20[e]	0.9 ± 0.3	5.76[e]	0.24 ± 0.07	5.30[f]	3.0 ± 0.2
9.40[i]	0.9 ± 0.4	6.15[e]	0.07 ± 0.05[c]	5.80[e]	0.27 ± 0.02
10.40[i]	1.5 ± 0.6	9.67[i]	0.21 ± 0.07[c]	6.26[e]	0.18 ± 0.01[c]
11.02[i]	3 ± 1	9.80[i]	0.29 ± 0.03[c]	10.01[i]	0.31 ± 0.05
		10.14[i]	0.7 ± 0.2	10.33[i]	1.0 ± 0.2
		10.24[i]	1.2 ± 0.2	10.91[i]	1.1 ± 0.6
		10.64[i]	1.5 ± 0.4		
		10.98[f]	1.8 ± 0.4		

[a] Solvent contains 30% THF, $\mu = 0.5$ M (NaCl), $T = 21$ °C.
[b] Values correspond to the single kinetic process experimentally detected under these conditions.
[c] Values listed correspond to the faster process, unless indicated otherwise, since values for the slower process do not show any significant buffer dependence.
[d] Errors given correspond to the standard deviation.
[e] Phosphate buffer.
[f] Acetate buffer.
[g] Buffer rate constant for slower process $= (0.18 \pm 0.04) \times 10^5\,M^{-1}\,s^{-1}$.
[h] Buffer rate constant for slower process $= (0.17 \pm 0.03) \times 10^5\,M^{-1}\,s^{-1}$.
[i] Carbonate buffer.

catalytic rate constant for acetic acid increases in the order **FHDPT**(a) < **MFDPT**(a), whereas data for carbonate buffer indicate that the catalytic rate constant for carbonate ion increases in the order **MFDPT**(a) < **FHDPT**(a). These trends can be easily rationalized in each case in terms of an increase in N-1 basicity and H—N-3 acidity, respectively, due to the electronic effects of X (i.e. H or CH_3O). Moreover, these trends fully agree with the general trend previously observed for symmetrical 1,3-diaryltriazenes, i.e. acid catalysis becomes dominant as the electron-donating character of the aryl groups increases, whereas base catalysis becomes predominant as the electron-withdrawing character of the aryl groups increases.[7]

Since the substituents of the substrates of this study are in different rings, a quantitative structure-reactivity analysis of the data for restricted rotation requires a multiple-substituent Hammett equation as given by Eqn (4):[12]

$$\log k_{rot}^{XY} = \log k_{rot}^{HH} + \rho_{Im}\sigma_{Im} + \rho_{Am}\sigma_{Am} \qquad (4)$$

where k_{rot}^{HH} represents the rate constant for *s-cis* to *s-trans* conversion of *cis*-1,3-diphenyltriazene (i.e. X = Y = H), σ_{Im} and σ_{Am} are the σ values for substituents at the phenyl rings bonded to the diazo (N-1) and amino (N-3) sites, respectively, and ρ_{Im} and ρ_{Am} are the ρ values for N-1 and N-3, respectively. In Fig. 4, the six rate constants for restricted rotation obtained in this study (closed circles) are plotted together with the six values obtained previously with symmetrical triazenes (open circles, X = Y = CH_3O, CH_3, H, Cl, CF_3 or CN).[7] The quality of the two-variable fitting is very good ($R = 0.992$). Equation (4) implies that the presence of a substituent in one ring does not disturb the sensitivity of the reaction to the substituent in the other ring, i.e. the cross-interaction is negligible, as one would expect for a reaction with minimal change in the distance between substituent sites at the rate-controlling step.[13] Furthermore, a negligible cross-interaction is in agreement with the fact that a good linear correlation is obtained with data for symmetrical triazenes (as clearly represented by the set of open circles lined up on a diagonal line). A double-variable curve fitting leads to values of 4.68 ± 0.03, -1.93 ± 0.08 and 0.82 ± 0.08 for $\log k_{rot}^{HH}$, ρ_{Im} and ρ_{Am}, respectively. The negative sign of ρ_{Im} implies the electron density on N-1 *decreases* on rotation, whereas the positive sign of ρ_{Am} implies the electron density on N-3 *increases* on rotation. These results can easily be explained in terms of the 1,3-dipolar resonance model [Eqn (3)]. Rotation around the N-2—N-3 bond reduces electron delocalization along the nitrogen chain by precluding conjugation. Consequently, the electron density at N-1 decreases and that of N-3 increases on going from ground state to transition state. The absolute value of ρ_{Am} is clearly lower than that of ρ_{Im}, which indicates that the restricted rotation is more sensitive to the electronic character of the aryl group attached to N-1 than to that of the aryl group bonded to N-3, as initially inferred from studies on symmetrical 1,3-diaryltriazenes.[7] Although no reaction constant for restricted rotation in *cis*-triazenes was available prior to our investigations, it is interesting that the ρ_{Im} value determined in this study is comparable to the ρ values obtained for restricted rotation in *trans*-1-aryl-3,3-dialkyltriazenes in organic solvents (i.e. -1.95 for 1-aryl-3,3-diethyltriazenes[14] and -2.01[15a]/-2.1[15b] for 1-aryl-3,3-dimethyltriazenes).

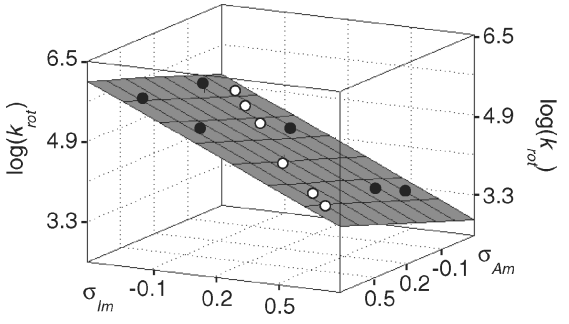

Figure 4. Double-variable fitting of the rate constants for restricted rotation in unsymmetrical (●) and symmetrical (○) *cis*-1,3-diphenyltriazenes to a multiple-substituent Hammett equation

In summary, we have investigated substituent effects on the isomerization of unsymmetrical disubstituted *cis*-1,3-diphenyltriazenes. The thermal *cis*-to-*trans* isomerization, as in the case of symmetrical disubstituted 1,3-diphenyltriazenes, involves a 1,3-prototropy catalyzed by general acids and general bases; the catalysis increases as the difference in the strength of the Brønsted catalyst and the substrate increases. Moreover, a comprehensive treatment of rate constants for rotation around the N-2—N-3 bond allows us to provide the first documented ρ_{Im} and ρ_{Am} values for restricted rotation in *cis*-triazenes.

EXPERIMENTAL

Unsymmetrical *trans*-1,3-diphenyltriazenes were synthesized by coupling anilines/diazonium salts via the classical diazotization method with $NaNO_2$, as described in the literature.[16] All three substrates were purified by column chromatography and recrystallization; melting-points and ^{1}H NMR data for **MHDPT** and **FHDPT** are in excellent agreement with reported values.[16] Analytical data for all three substrates are available as Supplementary Material at Wiley Interscience.

Kinetic studies were carried out using 30:70 (v/v) THF–water as solvent. Aqueous buffers were prepared using analytical-grade salts, water purified in a Millipore apparatus and spectrophotometric-grade THF (EM, Omnisolv grade). The ionic strength of the solutions was kept constant at 0.5 M using NaCl are compensating electrolyte. The pH of the solutions was measured using a combination electrode that had been calibrated with standard aqueous buffers.

Laser experiments were carried out using a Q-switched Nd:YAG laser (Continuum, Surelite I) operated at 355 nm (4–6 ns pulses, <30 mJ per pulse) for excitation. Further details on this laser system have been reported elsewhere.[17] Solutions were kept in quartz cells constructed of $7 \times 7\,mm^2$ Suprasil tubing. Transient spectra were collected under flow conditions in order to ensure the irradiation of fresh portions of sample by each laser pulse. For each solution, kinetic traces were recorded at different time domains (typically between 0.08 and 4 μs per point) and then combined for analysis; if necessary, traces were previously normalized to account for slight differences in signal intensities due to laser power fluctuations. All measurements were carried out at $21 \pm 1\,°C$. Values for the observed rate constants and for the Hammett reaction constants were obtained by using the general curve-fitting procedure of Kaleidagraph 3.6.2 from Synergy Software.

Acknowledgments

Financial support from the Natural Sciences and Engineering Research Council (NSERC) of Canada is gratefully acknowledged.

REFERENCES

1. Martin PJ. In *An Introduction to Molecular Electronics*, Petty MC, Bryce MR, Bloor D (eds). Oxford University Press: New York, 1995; Chapt. 6.
2. Dugave C, Demange L. *Chem. Rev.* 2003; **103**: 2475–2532.
3. (a) Suginome H. In *CRC Handbook of Organic Photochemistry and Photobiology*, Horspool W, Lenci F (eds). CRC Press: Boca Raton, FL, 2004; 94/1–94/55; (b) Diau EW-G. *J. Phys. Chem. A* 2004; **108**: 950–956; (c) Cembran A, Bernardi F, Garavelli M, Gagliardi L, Orlandi G. *J. Am. Chem. Soc*. 2004; **126**: 3234–3243.
4. Baro J, Dudek D, Luther K, Troe J. *Ber. Bunsen-Ges. Phys. Chem*. 1983; **87**: 1155–1161.
5. Scaiano JC, Chen C, McGarry PF. *J. Photochem. Photobiol. A: Chem*. 1991; **62**: 75–81.
6. Barra M, Chen N. *J. Org. Chem*. 2000; **65**: 5739–5744.
7. Chen N, Barra M, Lee I, Chahal N. *J. Org. Chem*. 2002; **67**: 2271–2277.
8. Taniguchi M, Uehara M, Katsura Y (Seiko Epson Corp.). Jpn. Kokai Tokkyo Koho JP 05 01,007, 1993; *Chem. Abs*. 1993; **118**: 223008q.
9. Borisov EV, Peregudov AS, Postovoi SA, Fedin EI, Kravtsov DN. *Bull. Acad. Sci. USSR, Div. Chem. Sci.* 1986; **35**: 499–502.
10. Lunazzi L, Panciera G, Guerra M. *J. Chem. Soc., Perkin Trans. 2* 1980; 52–55.
11. Mitsuhashi T, Simamura O. *Chem. Ind. (London)* 1964; 578–579.
12. Shorter J. In *Similarity Models in Organic Chemistry, Biochemistry, and Related Fields*, Zalewski RI, Krygowski TM, Shorter J (eds). Elsevier: Amsterdam, 1991; Chapt. 2.
13. Lee I. *Adv. Phys. Org. Chem*. 1992; **27**: 57–117.
14. Lippert Th, Wokaun A, Dauth J, Nuyken O. *Magn. Reson. Chem*. 1992; **30**: 1178–1185.
15. (a) Marullo NP, Mayfield CB, Wagener EH. *J. Am. Chem. Soc.* 1968; **90**: 510–511; (b) Akhtar MH, McDaniel RS, Feser M, Oehlschlager AC. *Tetrahedron* 1968; **24**: 3899–3906.
16. Day BF, Campbell TW, Coppinger GM. *J. Am. Chem. Soc*. 1951; **73**: 4687–4688.
17. (a) Sanchez AM, Barra M, de Rossi RH. *J. Org. Chem*. 1999; **64**: 1604–1609; (b) Barra M, Agha KA. *J. Photochem. Photobiol. A: Chem*. 1997; **109**: 293–298.